

Isomerization versus dissociation of phenylalanylglycyltryptophan radical cations

Xiaoyan Mu,^a Justin Kai-Chi Lau,^{b,c} Cheuk-Kuen Lai,^{a,b} K.W. Michael Siu,^{b,c}

Alan C. Hopkinson,^{b*} Ivan K. Chu^{a*}

^a*Department of Chemistry, The University of Hong Kong, Hong Kong, China*

^b*Department of Chemistry and Centre for Research in Mass Spectrometry, York University, 4700 Keele Street, Toronto ON, Canada M3J 1P3*

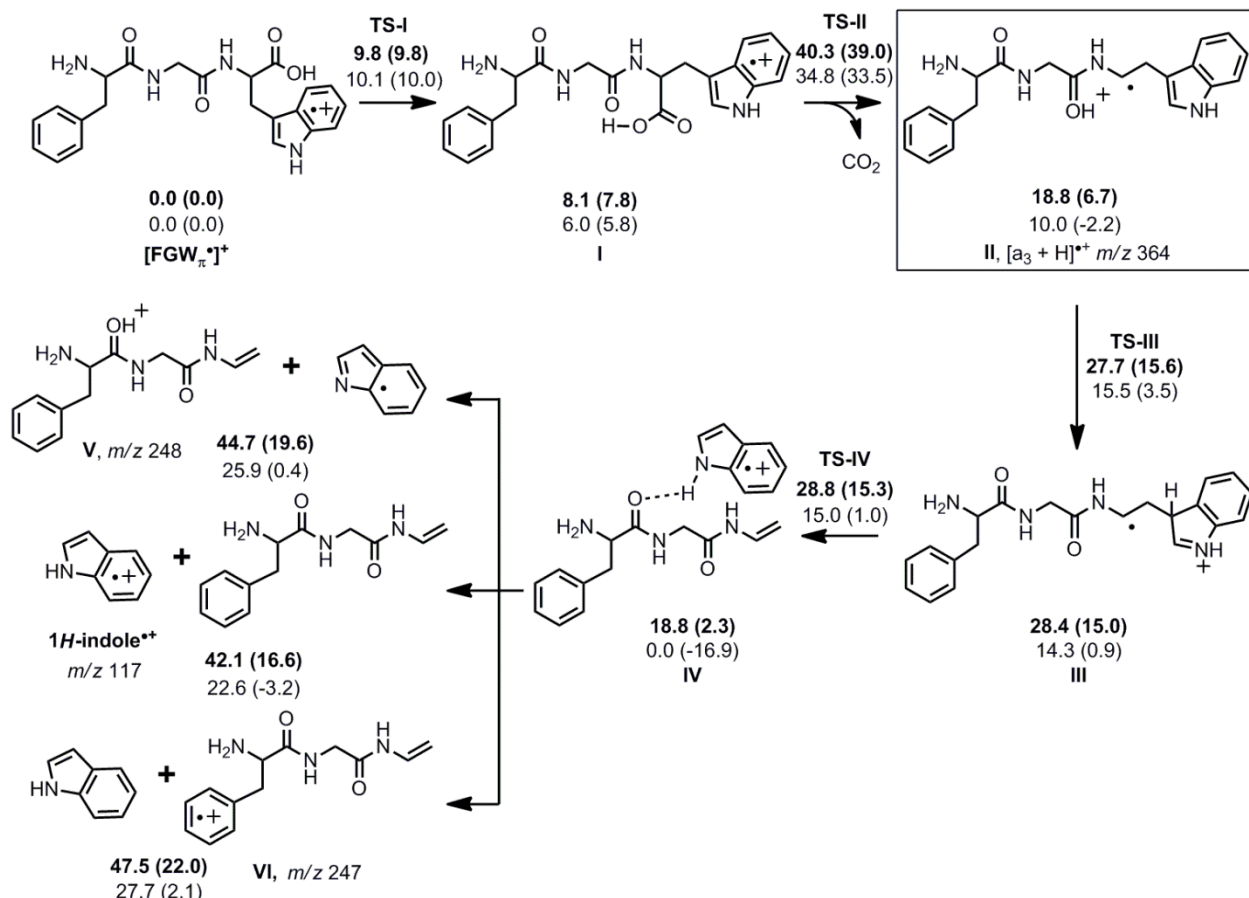
^c*Department of Chemistry and Biochemistry, University of Windsor, 401 Sunset Avenue, Windsor, ON, Canada N9B 3P4*

Supplemental information

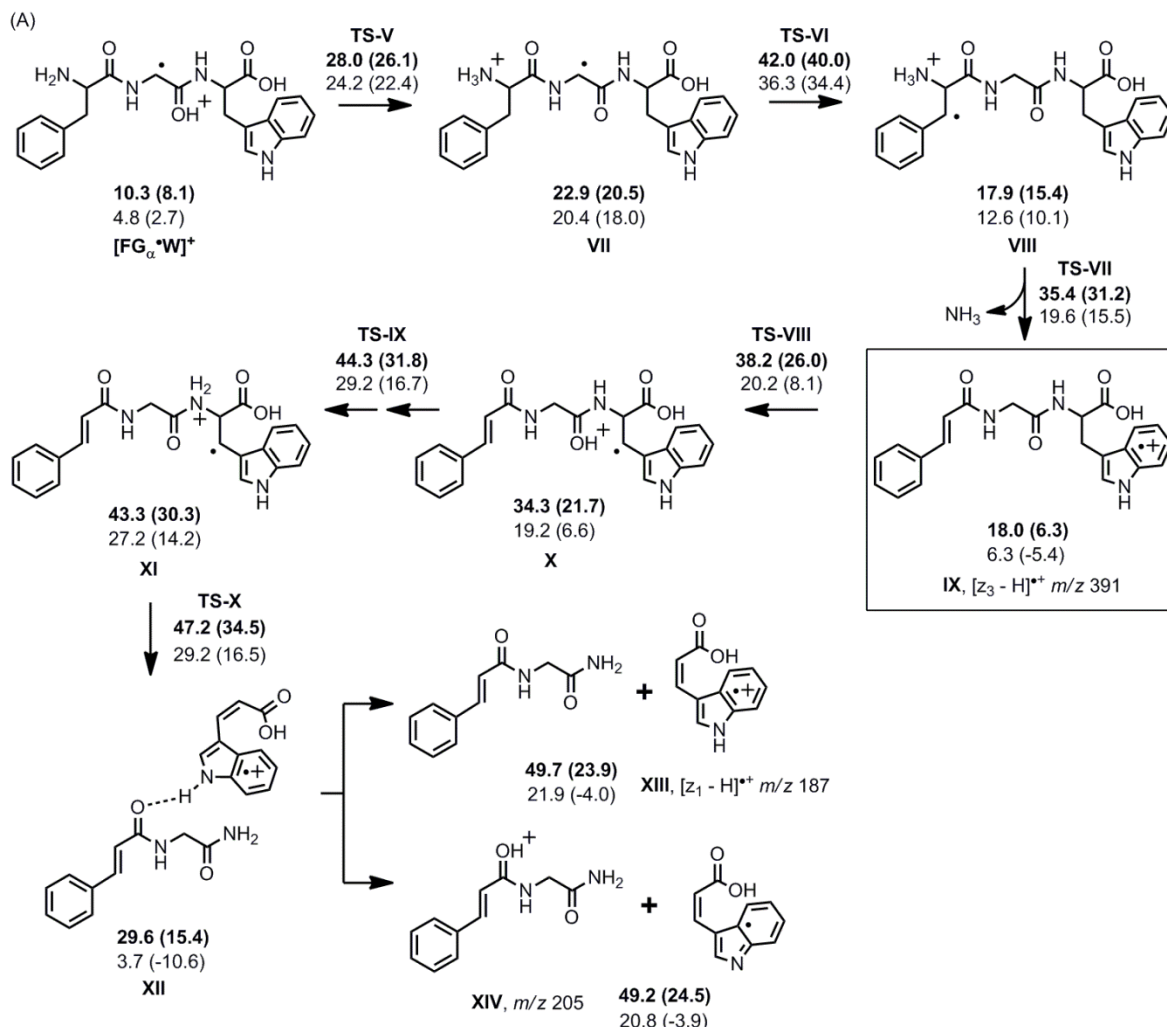
*Corresponding authors

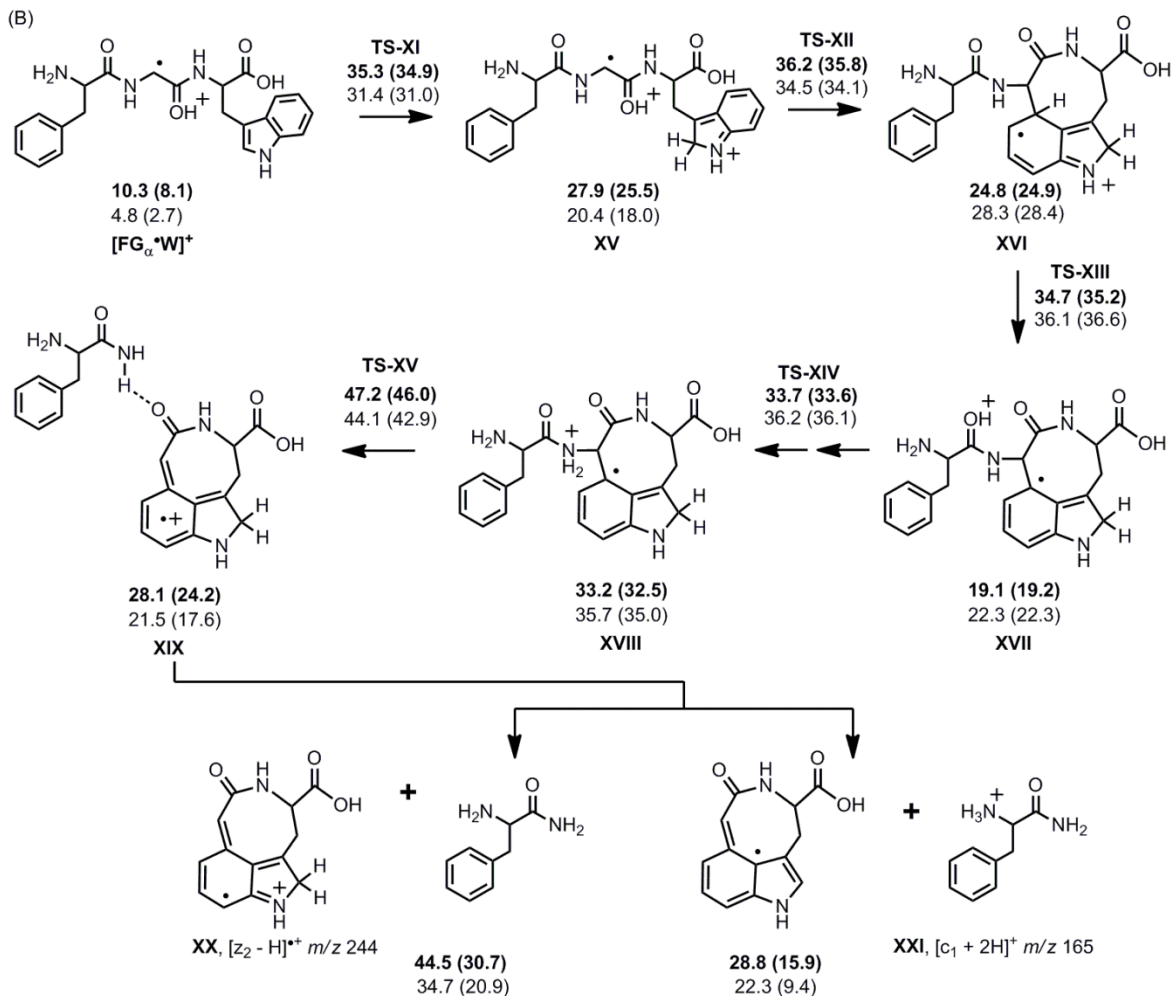
Email: ach@yorku.ca; ivankchu@hku.hk

Scheme S1. Detailed dissociation mechanism of $[FGW_{\pi}^{\bullet}]^+$. Upper numbers are the relative enthalpies (ΔH^0_0) and free energies (ΔG^0_{298} , in parentheses) determined at the M06-2X/6-311++G(d,p) level while the lower numbers are those determined at the B3LYP/6-31++G(d,p) level. All energies in kcal mol⁻¹ are relative to the $[FGW_{\pi}^{\bullet}]^+$ ion.

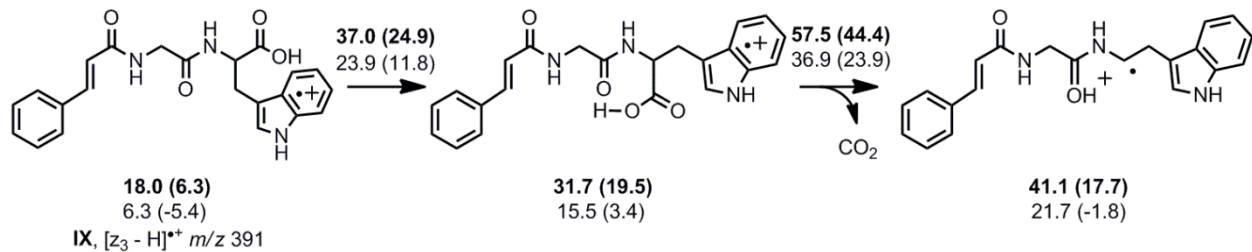


Scheme S2. Dissociation mechanisms of $[FG_{\alpha}^{\bullet}W]^+$ leading to the formation of (A) $[z_3 - H]^{\bullet+}$ and $[z_1 - H]^{\bullet+}$ ions and (B) $[z_2 - H]^{\bullet+}$ ion. Upper numbers are the relative enthalpies (ΔH^0) and free energies (ΔG^0_{298} , in parentheses) determined at the M06-2X/6-311++G(d,p) level while the lower numbers are those determined at the B3LYP/6-31++G(d,p) level. All energies in kcal mol⁻¹ are relative to the $[FGW_{\pi}^{\bullet}]^+$ ion.

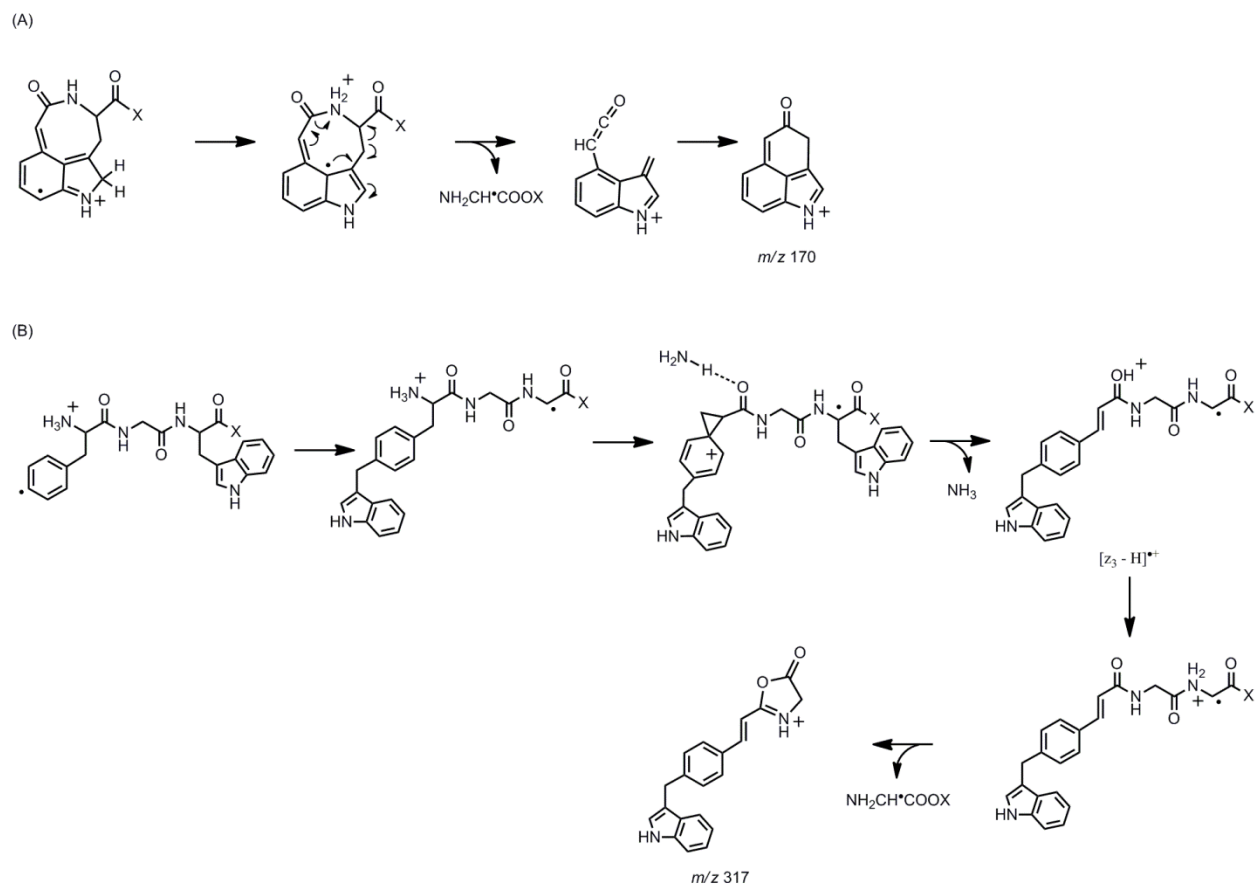




Scheme S3. Mechanism for the loss of CO₂ from [z₃ - H]^{•+} derived from [FG_α•W]⁺. Upper numbers are the relative enthalpies (ΔH°_0) and free energies (ΔG°_{298} , in parentheses) determined at the M06-2X/6-311++G(d,p) level while the lower numbers are those determined at the B3LYP/6-31++G(d,p) level. All energies in kcal mol⁻¹ are relative to the [FGW_π•]⁺ ion.



Scheme S4. Proposed mechanisms for the loss of NH₂CH[•]COOX from the (A) [z₂ - H]^{•+} ion derived from [FG_α•W]⁺ and (B) [z₃ - H]^{•+} ion derived from [F_ζ•GW]⁺.



Scheme S5. Detailed dissociation mechanism of $[F\zeta^*GW]^+$. Upper numbers are the relative enthalpies (ΔH°_0) and free energies (ΔG°_{298} , in parentheses) determined at the M06-2X/6-311++G(d,p) level while the lower numbers are those determined at the B3LYP/6-311++G(d,p) level. All energies in kcal mol⁻¹ are relative to the $[FGW_\pi^*]^+$ ion.

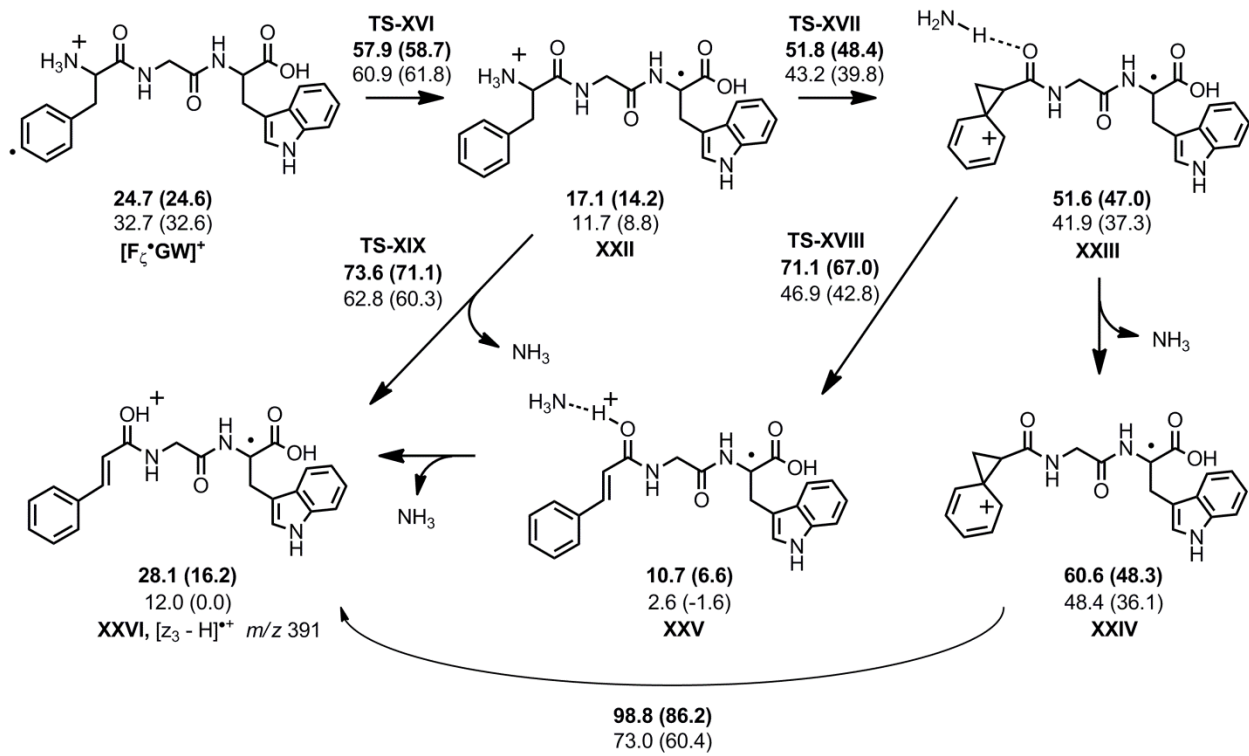


Figure S1. CID spectra of (A) $[\text{FAW}_\pi^\bullet]^+$ and (B) $[\text{FAW}_N^\bullet]^+$ radical cations

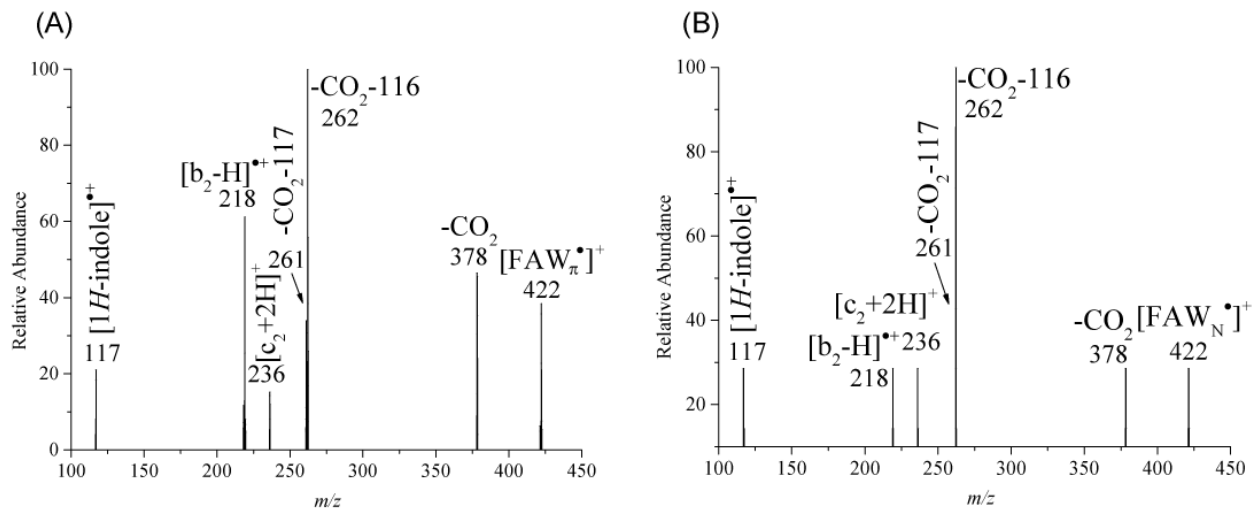


Figure S2. CID spectrum of $[\text{b}_3 - \text{H}]^{\bullet+}$ radical cation derived from $[\text{F}_\zeta\text{GW}]^{\bullet+}$

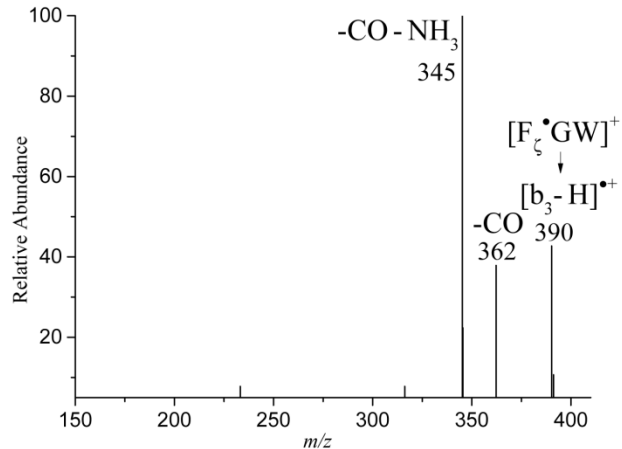


Figure S3. CID spectra of $[GA_{\alpha}^{\bullet}W]^+$, $[AG_{\alpha}^{\bullet}W]^+$, $[GG_{\alpha}^{\bullet}W]^+$, $[GG_{\alpha}^{\bullet}W\text{-OMe}]^+$ as well as the $[z_2\text{-H}]^+$ derived from $[FG_{\alpha}^{\bullet}W]^+$ and $[GG_{\alpha}^{\bullet}W\text{-OMe}]^+$.

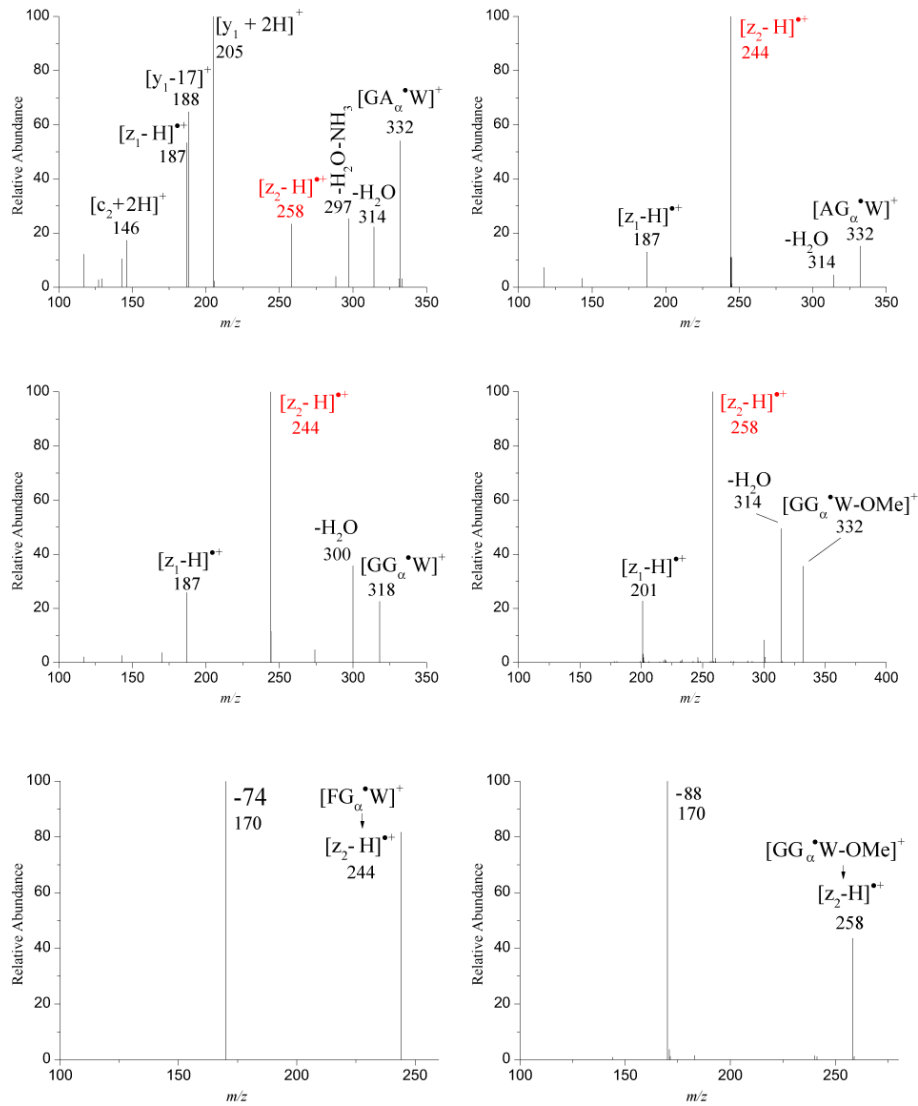


Figure S4. CID spectra of $[F\zeta\cdot GW_{(N-CH_3)}]^+$, $[F\zeta\cdot GW\text{-OMe}]^+$, $[F\zeta\cdot A_{(\alpha\text{-Me})}W]^+$ and $[F\zeta\cdot AW\text{-OMe}]^+$.

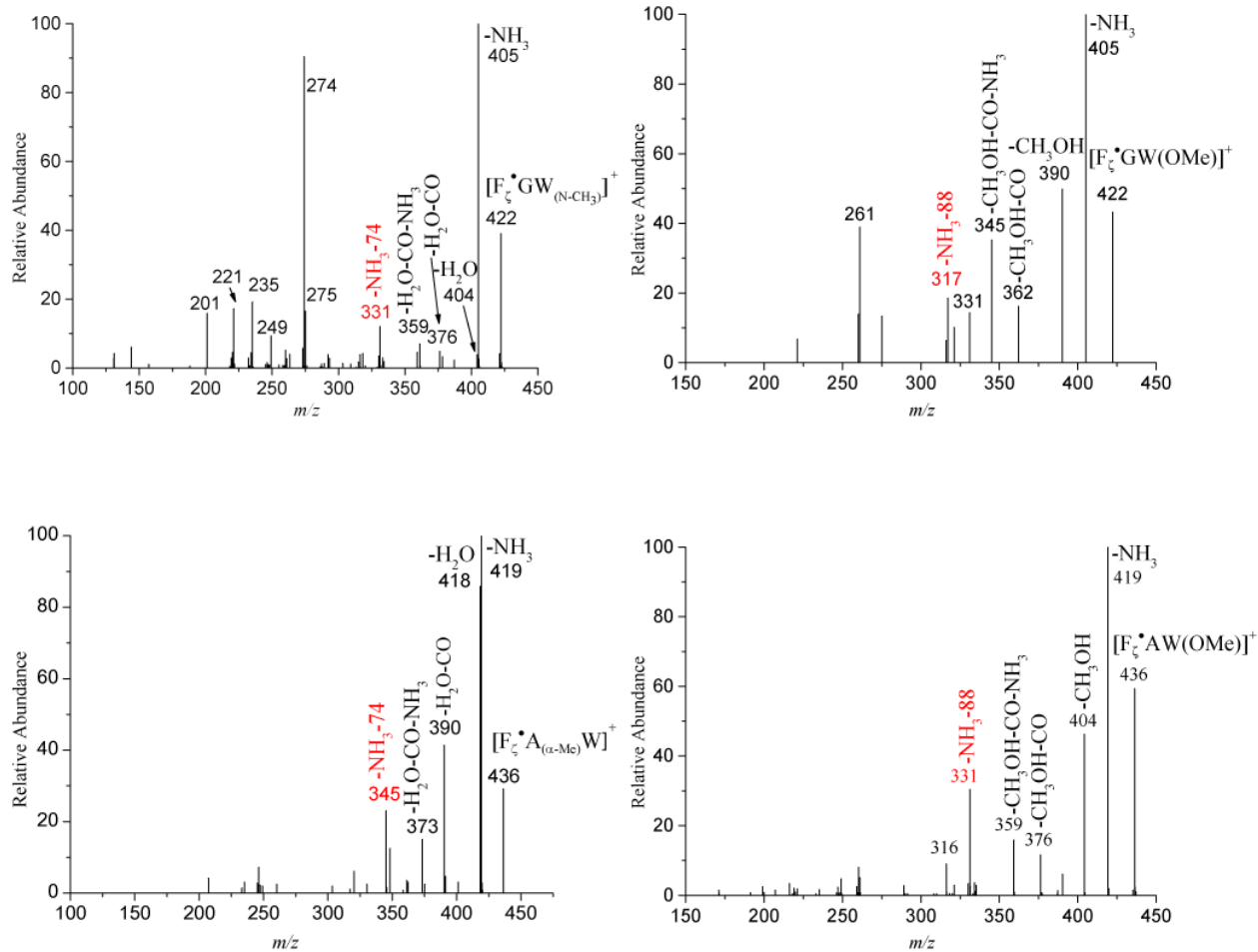


Table S1. Relative enthalpies (ΔH°_0) and free energies (ΔG°_{298} , in parentheses) of the minima and transition structures shown in Scheme 1-4 determined at various level of theory. All energies are in kcal mol⁻¹.

	M06-2X/6-311++G(d,p) ^a	B3LYP/6-311++G(d,p)	M06-2X/6-311++G(d,p)
[FGW _π •] ⁺	0.0 (0.0)	0.0 (0.0)	0.0 (0.0)
[FGW _N •] ⁺	24.0 (20.5)	17.0 (13.6)	24.4 (20.5)
[FG _α •W] ⁺	10.3 (8.1)	4.8 (2.7)	9.6 (7.1)
[F _ζ •GW] ⁺	24.7 (24.6)	32.7 (32.6)	23.9 (24.4)
TS-AB	31.1 (29.1)	28.1 (26.1)	31.3 (29.8)
TS-AC	45.5 (42.8)	34.6 (31.9)	45.8 (42.6)
TS-BC	47.1 (47.0)	42.4 (42.2)	45.8 (45.2)
TS-BD	61.3 (62.3)	59.6 (60.6)	61.0 (62.1)
I	8.1 (7.8)	6.0 (5.8)	7.2 (6.7)
II	18.8 (6.7)	10.0 (-2.2)	22.6 (10.4)
III	28.4 (15.0)	14.3 (0.9)	31.7 (18.6)
IV	18.8 (2.3)	0.0 (-16.9)	22.1 (6.5)
V	44.7 (19.6)	25.9 (0.4)	47.9 (22.1)
VI	47.5 (22.0)	27.7 (2.1)	48.5 (22.9)
VII	22.9 (20.5)	20.4 (18.0)	23.6 (20.9)
VIII	17.9 (15.4)	12.6 (10.1)	18.0 (15.0)
IX	18.0 (6.3)	6.3 (-5.4)	19.7 (7.8)
X	34.3 (21.7)	19.2 (6.6)	35.4 (22.5)
XI	43.3 (30.3)	27.2 (14.2)	43.4 (30.1)
XII	29.6 (15.4)	3.7 (-10.6)	31.5 (16.9)
XIII	49.7 (23.9)	21.9 (-4.0)	51.7 (25.0)
XIV	49.2 (24.5)	20.8 (-3.9)	50.4 (24.9)
XV	27.9 (25.5)	20.4 (18.0)	28.3 (25.8)
XVI	24.8 (24.9)	28.3 (28.4)	26.2 (25.8)
XVII	19.1 (19.2)	22.3 (22.3)	19.2 (18.7)
XVIII	33.2 (32.5)	35.7 (35.0)	34.1 (33.1)
XIX	28.1 (24.2)	21.5 (17.6)	27.8 (25.1)
XX	44.5 (30.7)	34.7 (20.9)	46.0 (32.0)
XXI	28.8 (15.9)	22.3 (9.4)	29.7 (16.0)
XXII	17.1 (14.2)	11.7 (8.8)	17.2 (14.4)
XXIII	51.9 (47.0)	41.9 (37.3)	52.6 (48.2)
XXIV	60.6 (48.3)	48.4 (36.1)	62.0 (49.4)
XXV	10.7 (6.6)	2.6 (-1.6)	11.3 (8.0)
XXVI	28.1 (16.2)	12.0 (0.0)	27.3 (15.6)
XXVII	51.6 (38.5)	34.1 (21.1)	52.9 (38.8)
XXVIII	60.2 (36.2)	42.1 (18.3)	55.3 (32.4)
XXIX	84.9 (60.4)	64.0 (39.5)	86.6 (61.3)

	M06-2X/6-311++G(d,p) ^a	B3LYP/6-31++G(d,p)	M06-2X/6-31++G(d,p)
TS-I	9.8 (9.8)	10.1 (10.0)	9.9 (9.9)
TS-II	40.3 (39.0)	34.8 (33.5)	40.1 (39.5)
TS-III	27.7 (15.6)	15.5 (3.5)	31.7 (18.6)
TS-IV	28.8 (15.3)	15.0 (1.0)	32.8 (19.0)
TS-V	28.0 (26.1)	24.2 (22.4)	28.2 (26.2)
TS-VI	42.0 (40.0)	36.3 (34.4)	41.3 (39.9)
TS-VII	35.4 (31.2)	19.6 (15.5)	39.5 (37.8)
TS-VIII	38.2 (26.0)	20.2 (8.1)	39.2 (26.3)
TS-IX	44.3 (31.8)	29.2 (16.7)	45.8 (32.8)
TS-X	47.2 (34.5)	29.2 (16.5)	48.4 (35.0)
TS-XI	35.3 (34.9)	31.4 (31.0)	34.9 (34.6)
TS-XII	36.2 (35.8)	34.5 (34.1)	37.8 (37.4)
TS-XIII	34.7 (35.2)	36.1 (36.6)	35.8 (36.0)
TS-XIV	33.7 (33.6)	36.2 (36.1)	34.3 (33.2)
TS-XV	47.2 (46.0)	44.1 (42.9)	46.4 (45.9)
TS-XVI	57.9 (58.7)	60.9 (61.8)	57.7 (57.8)
TS-XVII	51.8 (48.4)	43.2 (39.8)	52.6 (49.4)
TS-XVIII	71.1 (67.0)	46.9 (42.8)	73.7 (70.0)
TS-XIX	73.6 (71.1)	62.8 (60.3)	73.1 (70.0)
TS-XX	52.5 (39.9)	34.7 (22.1)	52.3 (39.6)
TS-XXI	85.5 (72.5)	68.1 (55.1)	85.3 (73.4)
TS-XXII	78.4 (63.8)	61.0 (46.5)	76.8 (66.0)

^aSingle-point energies based on the geometry optimized at the B3LYP/6-31++G(d,p) level